Tensile testing of sheet metals at elevated temperatures with optical strain rate control

David Naumann [1*], *Marion* Merklein [1]

[1] Institute of Manufacturing Technology (LFT), Friedrich-Alexander-Universität Erlangen-Nürnberg, Egerlandstraße 13, 91058 Erlangen, Germany

Abstract. The manufacturing of sheet metal parts from lightweight alloys is often restricted due to limited formability of the applied materials at room temperature. To overcome this issue, thermally supported forming processes like hot forming are used. To map and predict the material behaviour in simulations, the materials have to be characterised at elevated temperatures. For the elasto-plastic behaviour, this typically is done by tensile tests. Thereby, dependent of the testing system, inhomogeneous temperature distributions are introduced to the sample unintentionally. This commonly known issue leads to an unintended increase of the strain rate during testing. Optical strain rate controlling (OSRC) is a new approach that enables the determination of the strain hardening behaviour of sheet materials at a constant true strain rate. Hence, in the scope of this contribution, the titanium alloy Ti-6Al-4V, is investigated at temperatures between 600 °C and 900 °C, at strain rates of up to 0.1 s^{-1}. The tensile tests were carried out on a Gleeble 3500 GTC simulator together with an ARAMIS 3D DIC system for the in-situ strain measurement. The deviation of the strain rate evolution was improved up to fourfold by using the OSRC method in comparison to the conventional testing procedure.

Keywords: tensile test; Gleeble; DIC; strain rate.

1 Introduction

Comprehensive and precise mechanical characterisation is a key enabler for predictive numerical forming simulations. Especially the strain hardening behaviour of sheet metals is a main aspect of material cards. There are many different characterisation tests available to measure the hardening behaviour under different stress and strain states. The most common one is the uniaxial tensile test due to its international standardization, the high comparability and of course the simple stress state during uniform elongation. The main disadvantage of the uniaxial tensile test is its relatively low uniform deformation. This weakness gets even more pronounced by testing at elevated temperatures, which is mandatory, if the investigated process demands it. Nevertheless, in order to obtain valid results for the hardening behaviour beyond the onset of diffuse necking, different methods have been presented in the past. It is emphasised that this article refers to diffuse, not local necking.

Mechanical characterisation at elevated temperatures poses various challenges for conventional testing methods. These can be divided into two branches. One belongs to the elevated temperature itself and one belongs to the available testing systems. Both groups are presented in the following.

1.1 Mechanical characterisation at elevated temperatures

Li and Ghosh [1] investigated the tensile deformation behaviour for three different aluminium alloys in the temperature range between 200 °C and 350 °C. Hereby, an influence of the temperature on the end of uniform elongation was identified. In dependence of the alloy composition, the uniform deformation was increased or decreased. This influence also was observable for the strain rate, but again without a strict trend. In addition Li and Ghosh stated, that the enhanced ductility of tensile tests at elevated temperatures can be contributed to the post-necking deformation. Hence, the possibilities of an enhanced and improved characterisation at elevated temperatures can be assigned to the post-necking behaviour. If it is possible to get information out of this specific area, more data is available to increase the fitting quality of the underlying constitutive model for simulations. Coelho and Thuillier [2] investigated the tesnile behaviour of a titanium alloy in so called Gleeble tensile tests at elevated temperature. Thereby they point out, that it is important to fit the evaluation area and the gauge length of the sample to the testing requirements, especially, if the testing systems introduce temperature gradients to the sample. This impact is introduced in the following section. Correspondingly, one major influence presented, is the discussed increase

* Corresponding author: david.naumann@fau.de

of strain rate in the centre of the specimen as a result of the inhomgenities.

Not only the material, but also the method for strain evaluation is from great relevance to obtain valid data. Therefore, many evaluation methods have been presented in the past. For a full field, three-dimensional strain measurement, it is state of the art to use a camera system based on digital image correlation (DIC). This enables local strain measurements which facilitates true strain investigation assuming volume constancy which is given by [3]:

$$0 = \varepsilon_1 + \varepsilon_2 + \varepsilon_3 \quad (1)$$

Whereby ε are the plastic strains in the primary directions. To account for the evolution in stress state, from uniaxial to three-dimensional state with the beginning of diffuse necking. Hoffmann and Vogl [3] presented a method for the utilisation of a 3D-DIC system to obtain local strain and stress data for the first time. With that, it is possible to determine true stress-strain-curves in tensile tests beyond the point of diffuse necking. Merklein and Gödel [4] thereby suggest the usage of an effective strain notation like given in equation (2):

$$\varepsilon_{vM} = \sqrt{\frac{2}{3}(\varepsilon_1{}^2 + \varepsilon_2{}^2 + \varepsilon_3{}^2)} \quad (2)$$

Hence, an easy method is given to provide material data for simulations as well as to compare the flow behaviour of sheet metals between different characterisation tests with varying stress conditions. Still unsolved, is the uncontrolled increase of strain rate in the area of strain localisation which is caused by either constant crosshead speed of the testing machine or the integral control length, which is defined by the gauge length of the specimen. The last mentioned corresponds to the method A1 of the ISO 6892-1 standard, which specifies an integral strain measurement between two points along the gauge length. This phenomenon is well described in the literature e. g., by Coelho and Thuillier [2].

1.2 Testing systems and specimen geometry

An even more significant influence on the strain gradients during tensile testing is introduced by the testing systems themselves. Due to its capabilities in terms of achievable temperatures as well as high testing speeds, Gleeble simulators are widely used, not only for characterisation s tasks intended for constitutive modelling, but also for process simulations. One disadvantage is given by its combination of electrical resistive specimen heating and cooled clamping jaws. Since the electrical energy, which is converted into heat in the sample by joule heating, is extracted by the clamping of the sample, an equilibrium is established that leads to a temperature gradient along the longitudinal axis of the sample. The highest temperature occurs in the centre of the sample, or more generally, in the area furthest away from the cooled clamping [5].

Fig. 1. shows the typically dog bone-shaped tensile test geometry with its characteristic lengths of L_0 which correspond to the initial valid evaluation gauge length, L_C which represents the parallel length of the sample and $L_{clamping}$ which refers to the free span between the clamping jaws of the testing machine.

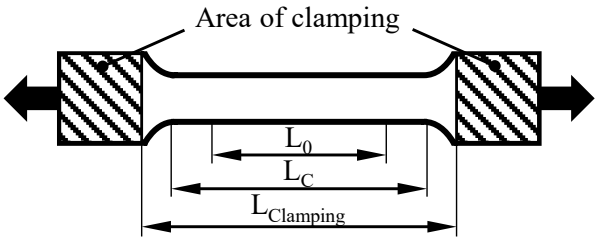

Fig. 1. Tensile test sample with characteristic gauge lengths

For conventional test setups, the displacement strain rate controlling (DSRC) procedure refers to L_c and the testing machine itself is considered to be stiff. Here, the strain rate is calculated by:

$$\dot{\varepsilon}(t) = \frac{v(t)}{L_c} \quad (3)$$

Thereby the change of the clamping length is measured by the crosshead position sensor which leads to an unknown strain state of the initial gauge length L_0. Even in a perfect setup, due to the fact that the areas of the radii are taking part in the deformation of the sample, a geometry-related strain inhomogeneity is introduced. Hence, the A1 procedure according the ISO standard 6892 recommends a strain rate controlling by considering integral elongation of the gauge length L_0.

Since most sheet metals have a temperature and strain rate sensitivity in their plastic deformation behaviour, such inhomogeneities implies challenges to characterisation tests as given in Fig. 2 for the yield stress. This shows the effect of an increasing strain rate on the determination of the yield stress of a material with positive strain rate sensitivity compared to a constant strain rate.

One approach, to determine constant, true strain rate material data from tensile tests with pronounced strain localisation, is given by local optical strain rate controlling. This is a further developed version of the optical strain rate control presented by Naumann and Merklein [6]. Aim of this contribution is therefore to investigate the impact of the testing method has on the determination of the true stress-strain behaviour of a titanium alloy at elevated temperatures.

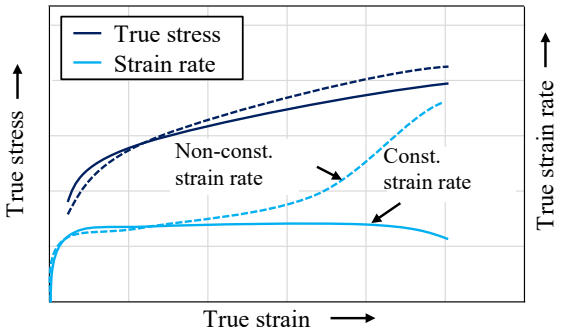

Fig. 2. Flow curve distortion introduced by strain rate variation

2 Methodology and experimental setup

2.1 Methodology

To investigate the improvement of the strain rate evolution during tensile testing as well as the hardening behaviour by utilising local optical strain rate control, tensile tests of the titanium alloy Ti-6Al-4V with a nominal sheet thickness of 1.5 mm are carried out at two different temperatures and strain rates from 600 °C to 900 °C and 0.01 s^{-1} to 0.1 s^{-1}. All parameter variations are carried out with OSRC and DSRC whereby the variations are repeated three times to obtain statistically relevant results. The curves shown, are selected but representative curves. To identify relations between the temperature distribution and the strain distribution during tensile testing, both are analysed.

2.2 Experimental setup

All tensile tests are carried out on a Gleeble 3500-HS GTC and conductive specimen heating at a rate of 20 °C/s. The samples are clamped by so called hot jaws, made out of stainless steel with a reduced contact area to the specimens in order to reduce the heat flow into the clamping and to obtain a more homogeneous temperature distribution. Conductive sample heating is chosen due to the possibilities of a process-oriented test procedure. For the optical strain measurement, an ARAMIS system consisting out of two CMOS-cameras with a resolution of 2.3 megapixel are utilised. The live-evaluation for the closed loop control was done with a workstation running the Software ZEISS Inspect 2023. The live-signal of the length change was transferred in terms of a 0…10 V analogue signal. A schematic overview of the used setup is given in Fig. 3.

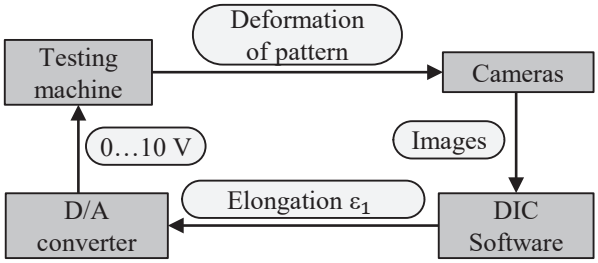

Fig. 3. Schematic diagram of the signal flow with the generalised elements of the closed loop control

For the closed control loop itself, a standard set-up consisting of a PID controller and a setpoint input is used. This setpoint is compared with the measured input value coming from the ARAMIS-system and a value deviating from zero triggers an adjustment of the crosshead speed. The difference between the DSRC and the OSRC strategy is therefore the actual value that is transferred to the control loop as measurement input.

Live evaluation strategy

Key point of the newly developed control strategy is the placement of the virtual extensometers to capture local strain phenomena. Main advantage of the virtual extensometer besides the fact, that they do not affect the sample itself, is the possibility to position them freely along the gauge length. Additionally, if more than one extensometer is used, an algorithm can decide, which measured value is passed to the closed loop control. As it is the aim of this work, to capture the maximum strain along the sample, which for tensile tests at elevated temperatures, usually is at the specimen centre, a line of extensometers is used as shown in Fig. 4. A configuration of nine extensometers with a length of 5 mm each, was applied.

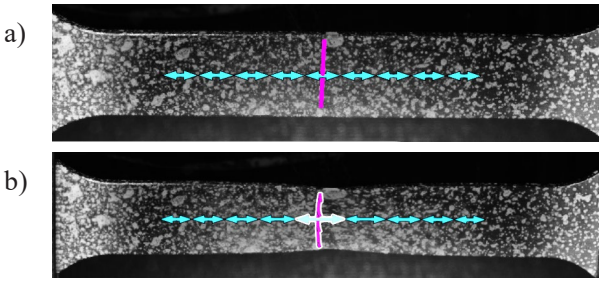

Fig. 4. Position of virtual extensometers (blue) on the tensile test specimen and section line for strain evaluation (violet) a) before start of the test b) during testing with highlighted extensometer selected according eq. 4

The selection of the extensometer to be controlled, follows the formula:

$$\varepsilon_{Controlling}(t) = \mathbf{max}(\varepsilon_1(t),\varepsilon_2(t), \ldots,\varepsilon_n(t)) \quad (4)$$

As a result, the area of maximum strains is detected automatically and thereby matched to the subsequent evaluation. For reference, conventional tensile tests at strain rates of 0.01 1/s and 0.1 1/s are carried out with an adaption of the crosshead speed according to Eq. 3 with an initial gauge length of 5 mm in order to keep the comparability to the optically controlled tests. Due to the increasing clamping length $L_{clamping}$ during the tensile tests, consequently the crosshead speed has to increase according eq. 3.

3 Results and discussion

3.1 Temperature evolution and distribution

At first, the temperature distribution of the investigated testing setup is analysed which is responsible for the introduction of inhomogeneous longitudinal strains. Fig. 5 provides an overview of the temperature distributions for two representative tests at 600 °C and 900 °C. Both testing temperatures introduce a near parabolic shape along the longitudinal axis of the specimens. This temperature distribution is well known and described for Gleeble tests. For materials that provide a decreasing yield strength by an increasing of temperature, the strain localisation will happen in the centre as described before. A deviation from this phenomenon can be caused by either a phase transformation, which is present for e. g., steels and titanium alloys, or an locally increase of the yield strength like blue brittleness for steels. Such phenomena is described by Seshacharyulu et al. [7]. They identified

a transient superplasticity mechanism at 0.01 s^{-1} of the fine-grained β-phase in the titanium alloy.

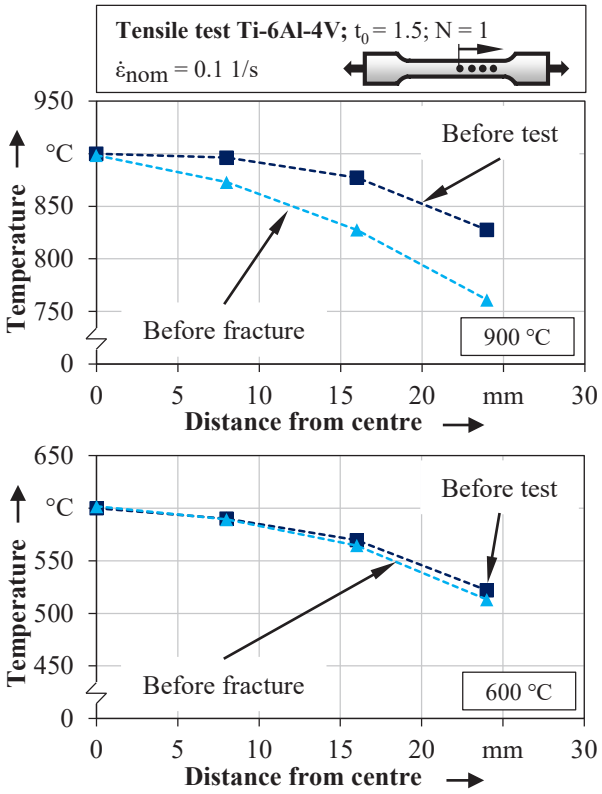

Fig. 5. Distribution of temperature along tensile test samples for 600 °C and 900 °C

Fig. 6 shows the temperature-time evolutions for trials conducted at 600 °C and 900 °C. After the nominal temperature in the centre is reached, a soaking time of 20 s follows to reach a near equilibrium state. After the beginning of the test, the temperature gradient increases up to the point of fracture. This increased gradient amplifies the inhomogeneities along the specimen. After the point of fractue, the temperature decreases rapidly, since the electric circuit is interrupted and the conductive heating is not possible anymore.

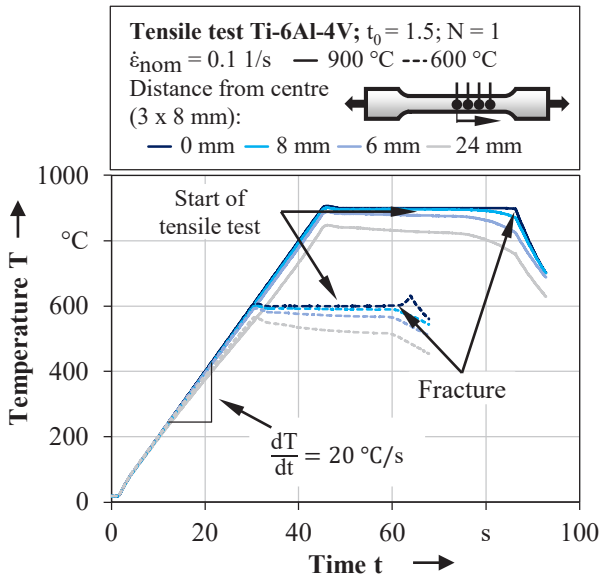

Fig. 6. Representative temperature-time evolutions in dependence of the position on the specimens

Due to the fact, that the temperature is controlled according the value measured at the centre, the respective temperatures fit the expected values sufficiently. However, the temperature decreases with an increasing distance to the centre. This temperature gap is 78 °C for the 600 °C trials and 73 °C for the 900 °C before tensile testing. Right before fracture, it is 88 °C and 138 °C at a distance of 24 mm to the centre (measured at the beginning of the test). This is the decisive factor for the strain inhomogeneities since the beginning of the test. To capture the true material behaviour at the desired temperature, strain evaluation is done along a transversal line at the specimen centre as shown in Fig. 4.

The strain hardening behaviour is significantly influenced by the applied testing method as displayed in Fig. 7. Both OSRC results for 0.01 s^{-1} and 0.1 s^{-1} show an increased flow resistance up to a true plastic strain of 0.3 and 0.15, respectively. Not only the absolute yield value is shifted, but also the characteristic course of the curve. The yield behaviour obtained by optical controled trials provides a much flatter curve, which means less hardening.

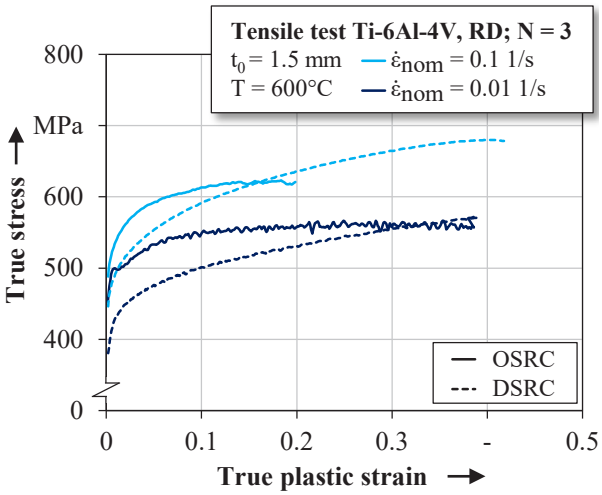

Fig. 7. True stress-true plastic strain curves for Ti-6Al-4V at 600 °C

Fig. 8 provides the corresponding true strain rate evolutions to the above given yield curves. For a higher comparability, the strain rates are given by normalized values. After a peak of close to two times the nominal strain rate, both OSRC trials match the nominal value at a true strain of about 0.03 for 0.01 s^{-1} and 0.08 for 0.1 s^{-1}. From there, the strain rates are kept constant until fracture is reached. The DSRC tests show a significantly lower strain rate of approx. 0.2-times the nominal value at the beginning. Thereafter, the strain rates increase constantly until breakage. The evolutions show an accelerated strain rate up to a two- or fourfold increase.

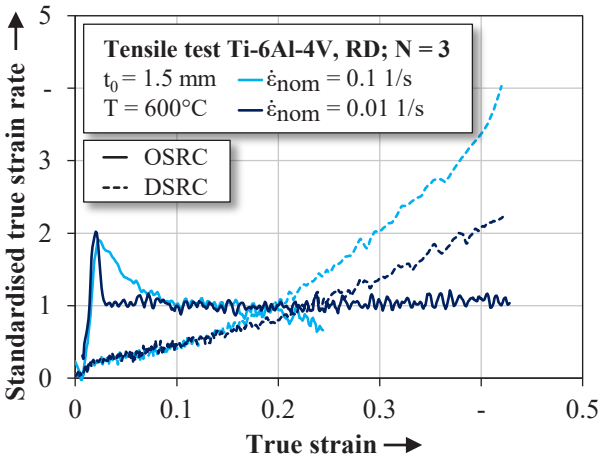

Fig. 8. True strain rate evolutions at 600 °C

For 900 °C testing temperature, an even more pronounced influence was identified. As shown in Fig. 9 both OSRC yield curves are not as smooth as the DSRC curves due to the elevated temperature, which introduces challenges to the optical strain measurement.

The characteristics of the DSRC trials show a typical strain hardening behaviour with an increasing yield stress but a decreasing slope. The opposite behaviour was found on the OSRC trials. Both investigated strain rates, high and low, provide the highest strength right after the initial yielding, whereby the yield stress reduces with increasing strain. The DSRC yield curves do not reach the level of the OSRC tests.

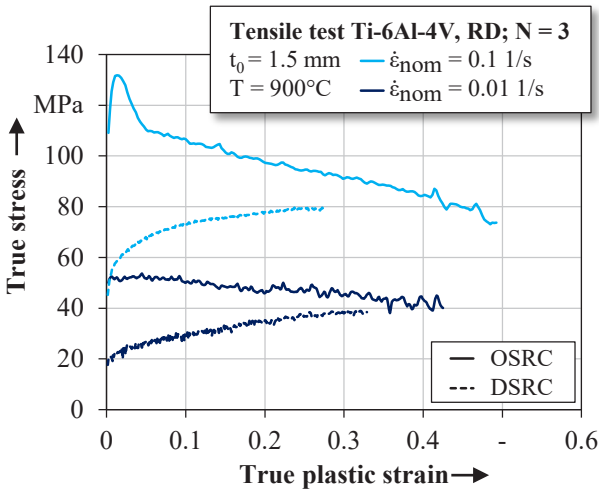

Fig. 9. True stress-true plastic strain curves for Ti-6Al-4V at 900 °C

The above identified higher yield stress of the OSRC tests can be attributed to the higher strain rates given in Fig. 10. But not only the higher absolute value of the strain rate is responsible, but in particular the evolution of the strain rate with its linear increase. This increase of strain rate causes the flow resistance from the DSRC tests to increase. On the one hand, the strain rate sensitivity of the investigated Ti-6Al-4V alloy is higher at 900 °C than at 600 °C and on the other hand, the higher temperature as well as the higher temperature gradient along the sample introduces a changed strain distribution. Thereby a wider range of the initial gauge length of the specimen takes part in the forming, which leads to lower strain rates in the DSRC tests. However, this initial strain rate deviation could be reduced by adapting the gauge length setup for the DSRC tests in a trial-and-error manor which is also known as open loop control. Nevertheless, the non-constant strain rate would be the same at another absolute strain rate level which causes the distortion of the yield curves.

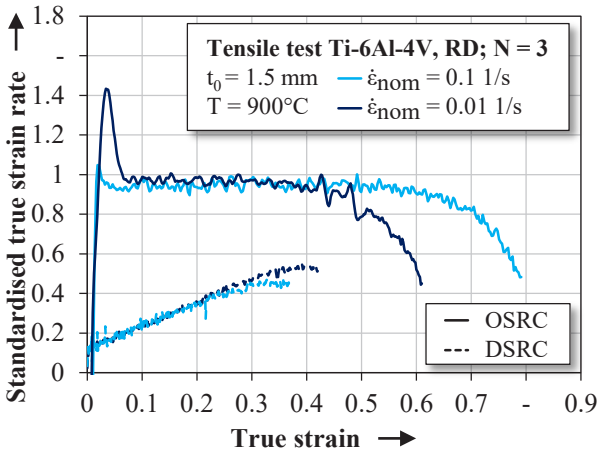

Fig. 10. True strain rate evolutions at 900 °C

The OSRC trials at 900 °C provide a lower strain rate peak at the beginning of the test in comparison to the 600 °C trials. Here, for the high strain rate of 0.1 s^{-1} the peak is negligible small whereby for 0.01 s^{-1} the peak reaches around 1.4-times the nominal strain rate. After the initial peak. Both evolutions meet the nominal value sufficiently precise.

It is striking that the strain rates decrease towards the end of the test at strains of around 0.4 for 0.01 s^{-1} and 0.5 for 0.1 s^{-1}. This is an indication that the controlled area of the virtual extensometer and the line for post-necking strain evaluation are not aligned anymore. If the strain localisation concentrates in the centre of the specimen, where the nominal temperature is kept constant, the strain rate also can be kept constant for the evaluation area which is fixed to the specimen centre in order to meet the expected temperature. If the strain localisation shifts away from the specimen centre, the strain rate decreases in the evaluated area. This can be explained by the fact, that the highest strain rates occur where the strains are the highest. This behaviour was observed in the 900 °C tests, where the samples fractured not symmetrically. This phenomenon can be attributed to the superplastic forming behaviour of the investigated titanium in combination to the temperature gradient. As Demirel and Karaağaç [8] investigated the superplastic forming behaviour of Ti-6Al-4V, the highest strains can be achieved for temperatures right below 900 °C. Thereby, the highest strains for the temperature gradient at a nominal temperature of 900 °C has to be outside the specimen centre.

4 Summary and Outlook

In the scope of this study, an innovative approach was presented to conduct tensile tests at elevated temperatures at locally constant true strain rates. By utilising a 3D-DIC system for in-situ optical strain

measurement as a strain input for a closed loop control, the strain rate was kept constant beyond the point of diffuse necking. This approach enables for the first time, a machine, temperature and material independent strain rate control scheme to investigate the elasto-plastic material behaviour in a wide range of strain rates, temperatures and temperature inhomogeneity. For the example of a hot formed Ti-6Al-4V alloy it was shown, that the testing method has a significant influence on the characterisation of the strain hardening. The strain rate evolution was improved by up to 200 % whereby a difference in the yield stress of over 80 MPa was identified. Additionally not only the level of the analysed yield stress changed, but also the way the alloy hardened with increasing strain. Conventional testing methods distort the characteristic yield stress evolutions and with that can cause an over- or underestimitation of the yield behaviour in dependence of the strain rate and temperature. This difference results from the changed strain rate which leads to a reduction of the flow resistance due to the positive strain rate sensitivity of the analysed material in comparison to the conventional testing procedures. The huge potential for local strain phenomena was shown, so further investigations should focus on the improvement of the strain rate evolution as well as the transferability to other materials like aluminium and steel. Also, an adaption and investigation for other characterisation tasks like e. g., nakajima tests and notched tensile specimens should be done. To capture the full potential of the presented characterisation method, the impact on FEA according a manufacturing process has to be evaluated.

Acknowledgement

This research was supported by the Bavarian Research Foundation (BFS) within the scope of the project 1565-22 “Optical strain rate control in material characterisation”. The authors are grateful to the industrial partners from AUDI AG, Carl Zeiss GOM Metrology GmbH, MATFEM Ingenieurgesellschaft mbH, Me-go GmbH and ZwickRoell GmbH & Co. KG for their support in the project. The authors would also like to show their gratitude to Mr. Mehmet Emre Şenses, who supported the experimental study within the scope of his function as a student research assistant. Lastly a special thanks goes to Dynamic Systems Inc. for their support.

References

1. D. Li and A. Ghosh, Mater. Sci. Eng. A **352**, 279 (2003)
2. B. Coelho and S. Thuillier, "On the use of the Gleeble® test as a heterogeneous test: sensitivity analysis on temperature, strain and strain rate," IOP Conf. Ser.: Mater. Sci. Eng., (2022)
3. H. Hoffmann and C. Vogl, CIRP Annals, **52**, no. 1, 217, (2003)
4. M. Merklein and V. Gödel, Int J Mater Form, **2**, 415 (2009)
5. K. Fu, H. Peng, K. Zheng, and S. Yuan, Int J Adv Manuf Technol, **125**, 1-2, 91 (2023)
6. D. Naumann and M. Merklein, "*Influence of an optical strain rate controlled tensile testing method on mechanical properties of sheet metals*," in Material Forming: ESAFORM 2024, 24-26 April 2024, France (2024)
7. T. Seshacharyulu, S. C. Medeiros, W. G. Frazier, and Y. Prasad, Mater. Sci. Eng. A, **284**, 1-2, 184, (2000)
8. M. Y. Demirel and İ. Karaağaç, "High-speed superplastic formability and deformation mechanisms of Ti6Al4V sheets," Mater. Sci. Eng. A, **866**, 144652 (2023)